

#### **OPEN ACCESS**

EDITED BY Anthony Lupo, University of Missouri, United States

REVIEWED BY

Marianne Bügelmayer-Blaschek, Austrian Institute of Technology (AIT), Austria Shrabani Tripathy, Washington University in St. Louis, United States

\*CORRESPONDENCE Gabriela G. Espejo ⊠ gabriela.espejogutierrez@unibe.ch

<sup>†</sup>PRESENT ADDRESS Thomas Röösli, SwissRe, Zurich, Switzerland

RECEIVED 15 July 2025 ACCEPTED 04 November 2025 PUBLISHED 28 November 2025

#### CITATION

Espejo GG, Stalhandske Z, Mühlhofer E, Röösli T, Brönnimann S, Bresch DN and Zischg AP (2025) From hazard to disruption: forecasting direct and indirect tropical cyclone impacts on infrastructure in Mozambique. Front. Clim. 7:1666586. doi: 10.3389/fclim.2025.1666586

#### COPYRIGHT

© 2025 Espejo, Stalhandske, Mühlhofer, Röösli, Brönnimann, Bresch and Zischg. This is an open-access article distributed under the terms of the Creative Commons Attribution License (CC BY). The use, distribution or reproduction in other forums is permitted, provided the original author(s) and the copyright owner(s) are credited and that the original publication in this journal is cited, in accordance with accepted academic practice. No use, distribution or reproduction is permitted which does not comply with these terms.

# From hazard to disruption: forecasting direct and indirect tropical cyclone impacts on infrastructure in Mozambique

Gabriela G. Espejo<sup>1\*</sup>, Zélie Stalhandske<sup>2,3</sup>, Evelyn Mühlhofer<sup>3</sup>, Thomas Röösli<sup>3†</sup>, Stefan Brönnimann<sup>4</sup>, David N. Bresch<sup>2,3</sup> and Andreas Paul Zischg<sup>1</sup>

<sup>1</sup>Mobiliar Lab for Natural Risks, Oeschger Centre for Climate Change Research (OCCR), Institute of Geography, University of Bern, Bern, Switzerland, <sup>2</sup>Institute for Environmental Decisions, ETH Zurich, Universitätstr, Zurich, Switzerland, <sup>3</sup>Federal Office of Meteorology and Climatology MeteoSwiss, Operation Center 1, Zurich, Switzerland, <sup>4</sup>Oeschger Centre for Climate Change Research (OCCR), Institute of Geography, University of Bern, Bern, Switzerland

Critical infrastructure (CI), such as healthcare facilities, schools, and the road network, plays a vital role in society by providing essential services that sustain the functioning of communities. Disruptions to this infrastructure can have profound consequences, affecting public health, safety, economic activities, and general well-being. Weather extremes, including tropical cyclones (TCs), are major drivers of such disruptions, causing widespread failures to power, communication, transportation, and healthcare. Forecasting the potential impact of weather events on these services in the weeks to days before landfall is crucial to enhance preparedness and enable effective anticipatory actions. Unlike previous efforts that focused primarily on estimating the potentially affected population, this research shifts attention to evaluating direct and indirect impacts on CI, and to capture the uncertain nature of impact forecasts depending on lead-time. The methodology, which relies entirely on open-source code and data, yields several metrics quantifying the impact of ensemble-based tropical cyclone (TC) wind forecasts on healthcare access, including the number of hospitals directly affected and the number of people indirectly affected due to disrupted access to healthcare facilities. We apply this approach to TCs Idai, Kenneth, and Freddy, which have struck Mozambique since 2019. The results highlight the extent of indirect effects on the population from infrastructure disruptions. Uncertainty arises from lead time, disruption threshold assumptions, and the challenge of capturing impact magnitude, especially for rapidly intensifying TCs. These findings underscore the importance of including indirect impacts into Impact-Based Forecasting (IBF) frameworks, which could enhance decision making. This research aligns with the development of IBF and situational awareness mechanisms promoted by the World Meteorological Organization (WMO). Building on this, the work supports international organizations in activating early warning protocols and delivering more targeted aid, such as financial resources, blankets, medical supplies, and volunteer personnel by identifying where hospitals are likely to be disrupted and which populations may lose access to healthcare. The visualizations generated further assist decisionmakers in prioritizing areas that require immediate support.

# KEYWORDS

impact-based forecast, critical infrastructure, lifelines, healthcare, open-source, CLIMADA, tropical cyclones, indirect impact

# 1 Introduction

Powerful tropical cyclones (TCs) are some of the most impacting phenomena in nature, with worldwide damages estimated to exceed 800 billion dollars (Collalti and Strobl, 2022). A large part of the destruction caused by these TCs comes from three core elements: high wind speeds, coastal flooding due to storm surges pushing water inland, and river flooding (Bakkensen et al., 2018; Park et al., 2013). As population grows and urbanization increases, coupled with rising asset values and a changing climate, lifeline services and critical infrastructure (CI) face increasing risk from natural hazards (Cremen et al., 2022; Dodman et al., 2022). Natural hazards such as TCs can lead to widespread failures in lifeline services such as power, communication, transportation, and healthcare (Svegrup et al., 2019). The impact of failures in CI becomes evident in the context of natural disasters such as Cyclone Freddy in Mozambique. This event impacted many people across a large geographical area. It is estimated that around 1,187,265 individuals were affected by the storm's initial and second landfalls in locations such as Inhambane, Gaza, Zambezia, Sofala, Tete, Niassa, and Manica. Reports detailed damages to 104 schools and 30 medical centers (ReliefWeb, 2023).

CI plays a vital role in society by providing essential services that are necessary for the functioning of communities. These infrastructures are not isolated entities but are multifaceted urban systems interconnected with various elements, as described by Gheorghe and Vamanu (2005) as a "metasystem". This metasystem is crucial for maintaining societal functioning as the interconnections ensure the smooth operation and resilience of urban environments. Disruptions to these systems can have far-reaching consequences, affecting public health, educational services, well-being, hinders emergency response and isolates communities far beyond areas that are directly affected by adverse weather events (Mühlhofer et al., 2024; Papilloud et al., 2024). Given this vital role, the need to protect CI has been recognized in global resilience frameworks. Initial steps in focusing on essential physical infrastructure, networks, and services have been considered in the IPCC Working Group II reports, especially in its sixth cycle (O'Neill et al., 2022). Recognizing the far-reaching implications of CI failures, policymakers have acknowledged the pressing importance of prioritizing infrastructure resilience. Consequently, this focus has been incorporated into various agendas, including the Sendai Framework for Disaster Risk Reduction 2015-2030 (United Nations Office for Disaster Risk Reduction, 2015), the Sustainable Development Goals (SDGs) (United Nations Statistics Division, 2023), and the International Federation of Red Cross and Red Crescent Societies (IFRC). Current research on modeling CI impacts primarily addresses direct effects, such as structural damages or physical disruption of basic services. Despite these efforts, there is often insufficient knowledge about the extent to which social facilities are exposed to natural hazards (Verschuur et al., 2024). This gap in knowledge highlights the importance of understanding the interdependencies between end-users and critical infrastructure (Mühlhofer et al., 2023a). Therefore, capturing patterns of people experiencing service disruptions based on forecast data can provide more targeted and decision-relevant information to decision-makers. This is particularly important as they require a methodology that visualizes and enhances the understanding of impacts while incorporating metrics and statistics that can be reproduced quickly and are user-friendly for operational purposes. Although policymakers recognized the need for early warning through international frameworks as EW4All initiative (World Meteorological Organization, 2023), there is still limited academic and practical work focused on impact forecasting, particularly for CI.

Data on exposure and vulnerability of critical infrastructure can be combined with hydro-meteorological forecasts to estimate impacts on healthcare, education, and road networks days or hours in advance of an adverse event. Open-source platforms such as CLIMADA operationalize this integration in line with the IPCC risk framework. CLIMADA has been applied across diverse use cases, including impact-based forecasting for winter windstorms (Röösli et al., 2021), economics of climate adaptation studies (Bresch and Aznar-Siguan, 2021), and global multi-hazard risk assessments and climate-change risk projections (Stalhandske et al., 2024; Meiler et al., 2025a). Further applications include human mortality (Lüthi et al., 2023), human displacement (Meiler et al., 2025b; Kam et al., 2024), infrastructure and basic-service disruption (Mühlhofer et al., 2023a), and ecosystem services (Hülsen et al., 2025).

Impact-based forecasting (IBF) is the field of research that aims to calculate impacts based on exposure, vulnerability and hazard forecast. Its goal is to reduce losses, optimize communication and facilitate timely decisions (World Meteorological Organization, 2021). Questions such as where, what, and when impacts will occur, as well as the magnitude of these impacts in a given region, can be addressed through IBF. This information supports decision-making, especially in cases where the forecaster lacks extensive experience with past events (Golding, 2022; Lazo et al., 2020). The WMO, with governments, science groups, and the Red Cross and Red Crescent Climate Center, collaborates to transition to impact-based forecasting (United Nations Office for Disaster Risk Reduction, 2015; World Meteorological Organization, 2021). According to the research gaps identified by Potter et al. (2025) and Mosimann (2024), IBF requires research in four key areas: (a) vulnerability models to understand how exposed elements respond to hazards. (b) near real-time computation of hazard footprints and impact calculations to support timely decisions; (c) understanding uncertainties within the value chain; and (d) cartographic visualization to present information clearly for better understanding by decision-makers.

Recent IBF applications span multiple hazards and outcomes: winter-windstorm building-damage forecasts in Switzerland (Röösli et al., 2021); a global TC-displacement IBF that explicitly analyses uncertainty along the IBF value chain (Kam et al., 2024); a Philippines housing-damage IBF showing that models using only global features did not underperform and reduced false alarms (Kooshki Forooshani et al., 2024); and a surrogate flood IBF for Switzerland enabling near-real-time impact prediction (Mosimann et al., 2024). Complementing these, a comparative study of a machine-learning and a damage-curve model revealed sensitivity to lead time and trigger thresholds (Sedhain et al., 2025). Despite this progress, important research gaps remain:

IBF has largely focused on direct impacts, often overlooking indirect societal effects and cascading consequences (Potter et al., 2025).

This study addresses the gap by focusing on the calculation of indirect impacts based on impact forecasting, aiming to capture service disruptions as accurately as possible using the best available estimates at the time of the event. Uncertainty is addressed through cartographic visualizations of best and worst case scenarios, along with their associated probabilities. Consistent with Early Action Protocols (EAP), we target a five-day pre-landfall horizon for anticipatory action; if the ECMWF ensemble identifies the storm later than five days, we start from the first detection, for Idai four days ahead, for Kenneth one day, and for Freddy five days. We argue that forecasting and visualizing indirect impacts can provide valuable additional information to support decisionmaking before an event occurs. We applied predefined vulnerability curves to estimate direct impacts, which are then combined with real-time forecasts from the European Centre for Medium-Range Weather Forecasts (ECMWF) to compute hazard footprints and their associated impacts. We demonstrated the application of this approach using the three most significant TCs that have affected Mozambique. However, the methodology is generic, the code is open-source, and the data is transferable, making the approach easily applicable to other countries, hazards, and CI, and fully replicable.

## 2 Materials and methods

The IBF framework for TCs in Figure 1 sketches the workflow to calculate direct infrastructure and population impacts, and indirect service disruption impacts using TC track forecasts. The process for calculating impact forecasts of people experiencing basic service disruptions begins with a classic natural hazard impact calculation pipeline, following the IPCC definition of risk (Field et al., 2014). We combine spatially explicit data on (a) hazard forecast, (b) exposure, and (c) vulnerability. Finally, to compute direct impacts in (d), we implement the data from (a), (b), and (c) using CLIMADA (Aznar-Siguan and Bresch, 2019), an open-source software widely used in the climate risk assessment community. In (e), we extend the direct impact forecast pipeline to estimate indirect impact forecasts by considering disruptions to critical services or lifelines referred to here as Indirect I in (e) Figure 1 which occur when critical infrastructure can no longer provide essential services to the population. Although deriving service level disruptions directly from structural damage remains a challenge (Schneider et al., 2025), we approximate that infrastructure is fully non-functional, or "disrupted," when the impact exceeds a threshold, which we define as a severe impact (Section 2.2). We then subset the infrastructure identified as disrupted and visualize the affected CI, along with the potentially impacted population due to service disruption, under Indirect II in (e) (Subsections 2.2.1 and 2.2.2). The results obtained in (d) serve as input for estimating the population affected by disruptions (e) to hospitals, schools, and road networks, using a nearest-neighbor approach and the methodology of the Sustainable Development Goals (SDG) indicator 1.4.1 from the Metadata on SDGs.

## 2.1 Impact forecast pipeline: input

Our approach follows the IPCC view of risk as the interaction of hazard, exposure, and vulnerability. We implement this with the CLIMADA risk platform, which separates (i) the hazard module, (ii) the entity module (an exposure module and an impact functions, i.e. vulnerability, module), and (iii) the engine module that combines the three components to compute impacts. In our case, the hazard is constructed from tropical cyclone ensemble forecasts, and we explicitly use 10 m sustained wind speed (from the ensemble) as the hazard intensity field. Exposure includes geolocated infrastructure and population. Vulnerability is represented by empirically derived vulnerability curves and category thresholds. The engine module maps each wind field onto exposure coordinates and evaluates asset-level impacts. The resulting impact is given by Equation 1 in Section 2.1.4. The subsections below describe how CLIMADA structures the hazard, exposure, and vulnerability inputs, and how the engine module integrates them to produce impact estimates.

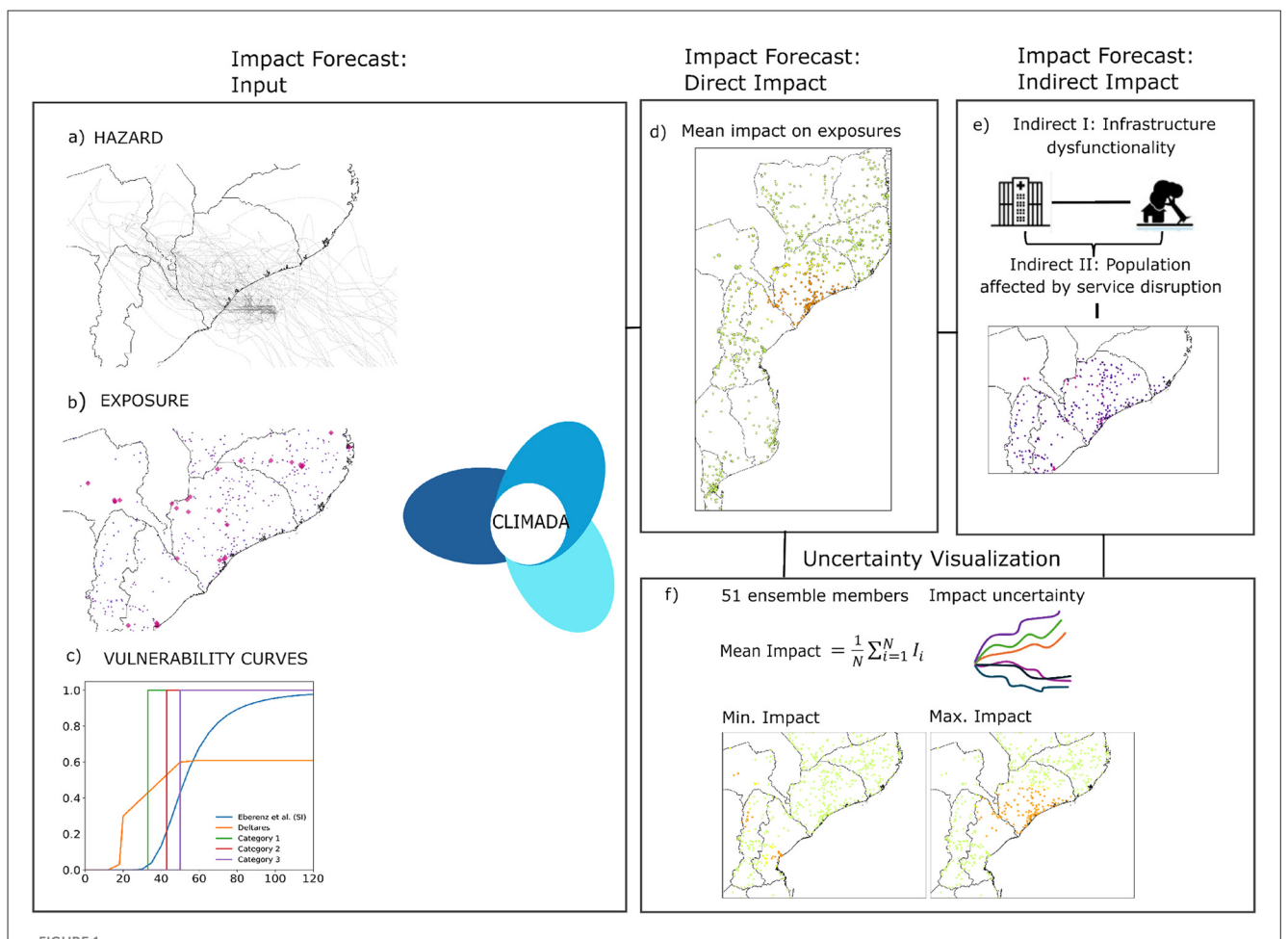
#### 2.1.1 Hazard

Hazard data can be derived from various sources, including forecasts, past events, climate projections, and even simulations, to generate probabilistic sets of events. We use ECMWF ensemble forecasts of sustained wind to estimate the number of affected infrastructure (Czajkowski and Done, 2014). The hazard data has been fetched from the ECMWF for TCs. While past records are not directly available in the ECMWF database, they can be accessed through the THORPEX Interactive Grand Global Ensemble (TIGGE). This forecast corresponds to the IFS Cycle 47r3, which encompass 51 ensemble members. The ECMWF Integrated Forecasting System includes track data consisting of forecasted positions (latitude, longitude), central pressure, environmental pressure, radius of maximum wind, and maximum wind speed, recorded every 6 h over a period of 240 hours. As the forecast data consist of the variables described above, preprocessing is necessary to obtain the wind field. This involves generating a static circular wind field for each track and calculating the translational wind speed. Several models have been developed for this purpose, and the pressure-wind model by Holland (Holland, 2008; Aznar-Siguan and Bresch, 2019) has been implemented in CLIMADA via the TropyCyclone module.

Hazard data were obtained from ECMWF tropical-cyclone (TC) forecasts; historical ensemble records are available via TIGGE. The ECMWF Integrated Forecasting System (IFS) provides a 51-member ensemble. For each member, the TC track product includes forecast positions (latitude, longitude), central pressure, environmental pressure, radius of maximum wind, and maximum wind speed, recorded every 6 hours over a period of 240 hours. Impact forecasts are generated at 150-arc-second ( 4 km) spatial resolution.

#### 2.1.2 Exposure

Exposure refers to the presence of assets or population geographically located within a specific area of interest. Exposure involves the quantification of infrastructure components using



Impact Forecast: The input consists of the interplay between (a) hazard forecasts, (b) exposure, and (c) vulnerability curves. In (d) Impact Forecast: Direct Impact, the impact is visualized based on the mean results across the 51 ensemble members. In (e), the plot shows infrastructure disruptions along with the population potentially affected. Finally, in (f), we illustrate the uncertainty inherent in impact forecast modeling by highlighting the differences among the highest-impact and minimum impact.

measurements such as spatial dimensions, encompassing both areas and basic value units (Mühlhofer et al., 2023a). Figure 1b illustrates the exposure data, which varies depending on the type of infrastructure and is represented by points (hospitals, schools and population) and lines (road networks). Exposure in the present study consist of hospitals, schools and roads networks retrieved from OpenStreepMap (CLIMADA, 2023), and high-resolution population data from WorldPop, with a resolution of 1 km at the equator (WorldPop Project, 2023). In the case of health facilities, we apply a categorization of hospital types based on reports developed by the Deltares Institute, documents from the World Bank Health Sector, and the Strategic Health Plan of Mozambique (Global Facility for Disaster Reduction and Recovery, 2023; Ministrio da Sade - Repblica de Moambique, 2007) To ensure data accuracy and cleanliness, geometric points with overlaps within 100 meters have been excluded. Road network data is grouped by highways, considering only main roads, while excluding roads labeled as "residential" and "unclassified". This procedure is necessary due to the occasional inaccuracies found in the data, as OpenStreetMap is an open-source platform developed by various users.

#### 2.1.3 Vulnerability

The definition of vulnerability varies across different disciplines. However, the Intergovernmental Panel on Climate Change (IPCC) report identifies two frameworks that share common causal factors of vulnerability. In disaster risk management, these factors are termed susceptibility/fragility and lack of resilience, while in climate change adaptation, they are referred to as sensitivity and lack of coping and adaptive capacities (Balica et al., 2009; Cardona et al., 2012). Vulnerability encompasses diverse dimensions, including socio-economic, environmental, and physical aspects. Building on this conceptual framing, a wide body of work has quantified infrastructure vulnerability in practice. On one side are engineering fragility/vulnerability functions for specific assets, often used directly for risk estimation, for example power-system assets under wind and flood (Ye et al., 2024). On the other side are data-driven, multi-indicator risk indices at high spatial resolution, for example block-level coastal flood risk using Random Forest (Yarveysi et al., 2025). While large-scale natural-hazard risk assessments for infrastructure are increasing, a recent cross-sector review highlights persistent gaps

in transferability and reproducibility, including limited treatment of multi-hazard and interdependencies, scarce open geolocated asset data, and challenges in scaling across geographies (Verschuur et al., 2024). Our approach is complementary: we do not derive new fragility models or socio-economic indices. Instead, we focus on the physical dimension risks to infrastructure using vulnerability functions also called fragility curves; termed "impact functions" in CLIMADA to map hazard intensity to structural damage (Figure 1c). To ensure broad applicability, we employ widely used structural-damage functions, the Eberenz and Deltares models (Eberenz et al., 2021; Mühlhofer et al., 2023b), and category thresholds consistent with the Saffir-Simpson scale. For example, a stepwise function can be applied to represent the distinct wind speed ranges of Categories 1, 2, and 3 of the Saffir-Simpson Scale. This means that the hazard intensity is discretized into levels based on defined wind speed thresholds. Further details on these vulnerability curves can be found in Supplementary Figure S1.

#### 2.1.4 Impact

Impacts are calculated using the CLIMADA risk assessment platform via the Impact module. Exposure and hazard data are overlayed, and the corresponding vulnerability curves are applied to compute impact and generate a cartographic representation. Since we use track forecast data, impacts are calculated for each of the 51 ensemble members. To visualize the direct impact on infrastructure and the uncertainty across the ensemble members, we used the mean impact calculated across all tracks. In contrast, to analyze the indirect impact, we applied the conditions described in the following Section 2.2.1.

The general impact at each exposed location k is calculated as:

$$x_k = H_k \cdot V_k(HE_k) \tag{1}$$

where  $x_k$  is the impact at location k,  $H_k$  is the hazard intensity, and  $V_k(HE_k)$  is the vulnerability as a function of local exposure and hazard.

For roads, which are represented as line strings, additional steps are introduced to calculate the mean impact per road. We disaggregate the line-strings into sections represented by points and take the average impact over the points belonging to each line, as shown by Equation 2. In this equation,  $\bar{x}_{ij,\text{osm}}$  is the average impact for a road segment identified by OSM\_id, calculated from the individual point impacts  $x_{ij}^{(k)}$ , with  $N_{\text{osm}}$  denoting the number of points along the segment.

$$\bar{x}_{ij,\text{osm}} = \frac{1}{N_{\text{osm}}} \sum_{l=1}^{N_{\text{osm}}} x_{ij}^{(k)}$$
 (2)

# 2.2 Impact forecast pipeline: indirect impact

# 2.2.1 Indirect I: infrastructure dysfunctionality

We extend the standard IBF by calculating not only direct impacts but adding disruption thresholds.

We assume that a disruption occurs when the following two conditions are met:

• Step 1: The impact value exceeds the structural disruption threshold of 0.20, based on the scale defined by previous studies in Australia. We adopt the risk categorization developed by Richter et al. (2018), where values equal to or above 0.20 indicate severe impacts. This condition is formalized in Equation 3, which maps the impact value  $x_{ij}$  at each point to a binary disruption indicator  $D_{ij}$ :

$$D_{ij} = \begin{cases} 1, & \text{if } x_{ij} \ge T_{\text{sd}} \\ 0, & \text{otherwise} \end{cases}$$
 (3)

where  $T_{\rm sd}=0.20$  is the structural disruption threshold.

• Step 2: A disruption is triggered if the proportion of ensemble members reporting an impact value  $x_{ij}$  exceeding the structural disruption threshold  $T_{\rm sd}$  at a given location is greater than or equal to a predefined alert threshold A. In this study, we use  $T_{\rm sd}=0.20$  as the structural disruption threshold and set the alert threshold A=0.10, meaning that an alert is issued if at least 10% of the ensemble members predict an impact value above 0.20 at the same location. This corresponds to at least 5 out of 51 ensemble members exceeding the condition  $x_{ij}>T_{\rm sd}$ , indicating a consistent signal of potential disruption across multiple forecast realizations.

We define the probability of disruption  $P_D$  as the ratio of the members of the ensemble that exceed the threshold to the total number of members of the ensemble:

$$P_D = \frac{N(x_{ij} > T_{\rm sd})}{N_{\rm ens}} \tag{4}$$

In our case, the probability of disruption becomes as follows:

$$P_D = \frac{5}{51} \approx 0.10 {(5)}$$

We do not claim these thresholds are the most suitable. The selected thresholds follow prior work and are set to a lower cut-off to reflect higher vulnerability in many countries of the Global South. Both the structural-disruption cut-off  $T_{\rm sd}$  and the alert share A are tunable operational parameters; their sensitivity is reported in the Supplementary Figure S8.

# 2.2.2 Indirect II: population affected by service disruption

The results obtained in Figure 1d Impact Forecast: Direct Impact and in Figure 1e Indirect I: Infrastructure dysfunctionality serves as input for estimating the population affected by disruptions to hospitals, schools, and road networks, using a nearest-neighbor approach when the exposure is represented as a geometric point. This methodology estimates the number of people who lose access to health and educational services due to infrastructure failure. Equation 6 describes the calculation of people experiencing basic service disruptions.  $h_i$  represents a hospital that has been damaged,  $p_j$  is the nearest population point obtained by minimizing the geodesic distance  $d(h_i, p_j)$ . The hospital location is then assigned to the nearest point of the impacted population  $imp_pole_{j^*}$ . This process ensures that every hospital is associated with its nearest population point.

For road network disruption, we used the metric from the Metadata on Sustainable Development Goals (SDGs) indicator 1.4.1. This involves calculating the population affected within a radius of 2 km of the disrupted road network. For these calculations, we use the subset of impacts obtained after applying one of the assumptions described in Section 2.2.1. The Equation 7 calculates the total affected population termed as (pp\_tot). Summing the impacted population  $imp_p(p_j)$  at each point  $p_j$  within 2 km of the road midpoint  $r_i$ . Interp( $r_i$ , 0.5) represents the midpoint of  $r_i$  and each population point is counted only once to avoid double counting.

$$pp_i = imp\_people_{j^*}, \quad where \quad j^* = arg \min_i d(h_i, p_j)$$
 (6)

$$pp\_tot = \sum_{i=1}^{n} \sum_{\substack{p_j \in \mathcal{P}_i \\ j \notin \mathcal{I}}} imp\_p(p_j), \text{ where}$$

$$\mathcal{P}_i = \{p_j \mid d(interp(r_i, 0.5), p_j) \le 2 \text{ km}\}$$
(7)

# 2.3 Impact forecast pipeline: uncertainty across the value chain

We quantify how uncertainty evolves across lead times and along the impact chain by computing ensemble-based spread statistics at each forecast step. All non-zero impact values across members and lead times are pooled and globally normalized to a common minimum and maximum, so differences reflect variability across forecasts rather than absolute magnitude. The spread of the ensemble is then summarized with the interquartile range (IQR), chosen for its robustness to outliers and its interpretation as the middle 50% of the predicted impacts. This yields a consistent basis for comparing uncertainty over time and across impact types (Supplementary material, Section 1.2).

# 3 Results

# 3.1 Impact forecast: direct impact visualization

To demonstrate the impact-based forecasting pipeline, we selected the three most significant TCs that affected Mozambique between 2019 and 2023. TC Idai reached Category 4 intensity on the Saffir-Simpson scale on 13 March 2019, weakening before making landfall near Beira as a Category 2 cyclone on 14 March at 2330 UTC (Nyongesa et al., 2024). Approximately one month later, TC Kenneth struck northern Mozambique, also reaching Category 4 intensity before making landfall on 25 April 2019 (Mawren et al., 2020). Three years later, Mozambique experienced the recordbreaking and longest-lasting TC Freddy, which made landfall twice. In the main paper, we focus on the second and most intense landfall of TC Freddy, which occurred on 11 March 2023 as a Category 5 cyclone (Liu et al., 2023). The results for TCs Idai and Kenneth are provided in the Supplementary Figures S2–S7. TC Idai caused the most significant damage, followed by TC Freddy, with estimated

283 economic losses of \$150 million (United Nations Office for Disaster Risk Reduction, 2023).

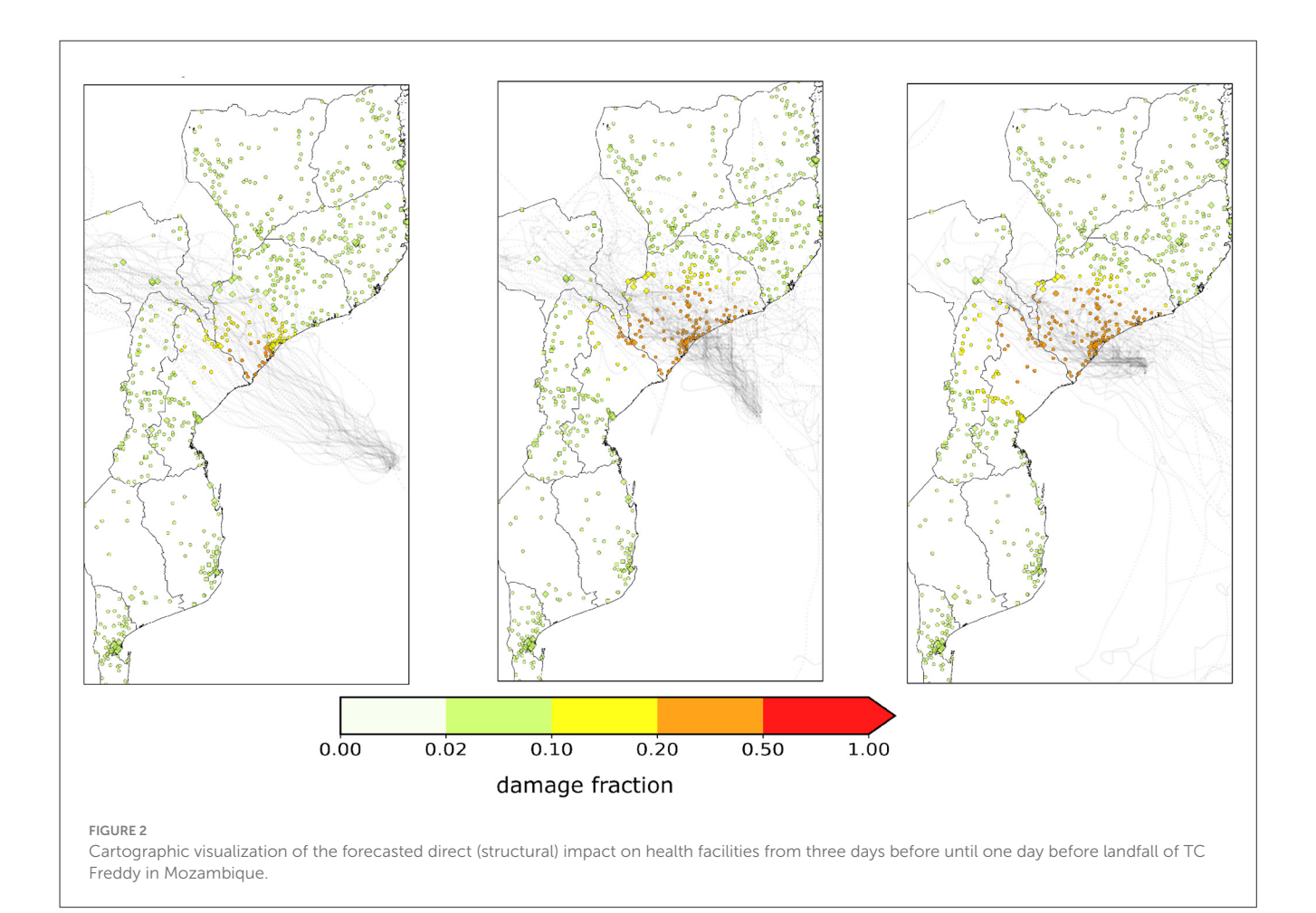
Figure 2 provides a cartographic representation of the Impact-Based Forecasting (IBF) results generated from the 51 ensemble members of the ECMWF. These maps show the predicted tracks of Tropical Cyclone Freddy, representing the best available forecast from three days before landfall until the cyclone reached Mozambique. Analogous plots for TCs Idai and Kenneth are provided in the Supplementary Figures S2 and S3. The exposure layer shown corresponds specifically to hospitals, highlighting the forecasted spatial distribution of impacts based on the hazardexposure-vulnerability framework described in Section 2.1. To represent hospital dysfunctionality, we used the mean impact value between the members of the ensemble at each location. This average reflects the expected severity and consistency of the impact, serving as a proxy for expected levels of disruption. Areas with higher mean values indicate a higher likelihood of disruption of hospital service due to TC Freddy. This visualization aims to help decision-makers quickly identify which hospitals are most likely to be affected, allowing for pre-emptive resource allocation and emergency planning.

To estimate the direct impacts on infrastructure and populations exposed to varying wind speeds, we provide a set of vulnerability functions. Decision-makers can select the appropriate function based on their expertise and the specific objectives of their impact assessments, as outlined in Section 2.1.3. Figure 2 presents a visual analysis of the impact status from three days to one day before landfall, revealing a shift in spatial patterns. These impact estimations are derived using the Deltares vulnerability function. Lower impacts are modeled three days before landfall, while higher impacts emerge as landfall approaches. These plots offer an initial basis for identifying potentially affected infrastructure and regions. However, the challenge of translating this information into societal consequences remains unresolved. For this reason, we incorporate estimations of indirect impacts in the subsequent steps of our analysis.

Figure 3 summarizes the number of hospitals, schools, and roads affected in Mozambique across the 51 ensemble members for each lead time (Step 1 in Section 2.2.1). To better capture the uncertainty across ensemble members, the figure presents the minimum, maximum, median, and mean number of affected elements for each lead time. Corresponding figures for Tropical Cyclones Idai and Kenneth are provided in the Supplementary Figures S4 and S5, respectively.

# 3.2 Impact forecast: indirect impacts

The novelty of this impact-based forecasting (IBF) research lies in the integration of indirect impacts within the value chain pipeline. This approach enables the provision of additional metrics to stakeholders, which may be useful for organizational tasks and informed decision-making. Beyond direct impact metrics such as the number of disrupted hospitals, schools, and primary road segments, we quantify indirect service disruption: (i) the population losing access to health care when a hospital is nonfunctional; (ii) the population losing access to education when a school is non-functional; and (iii) the population affected by loss of



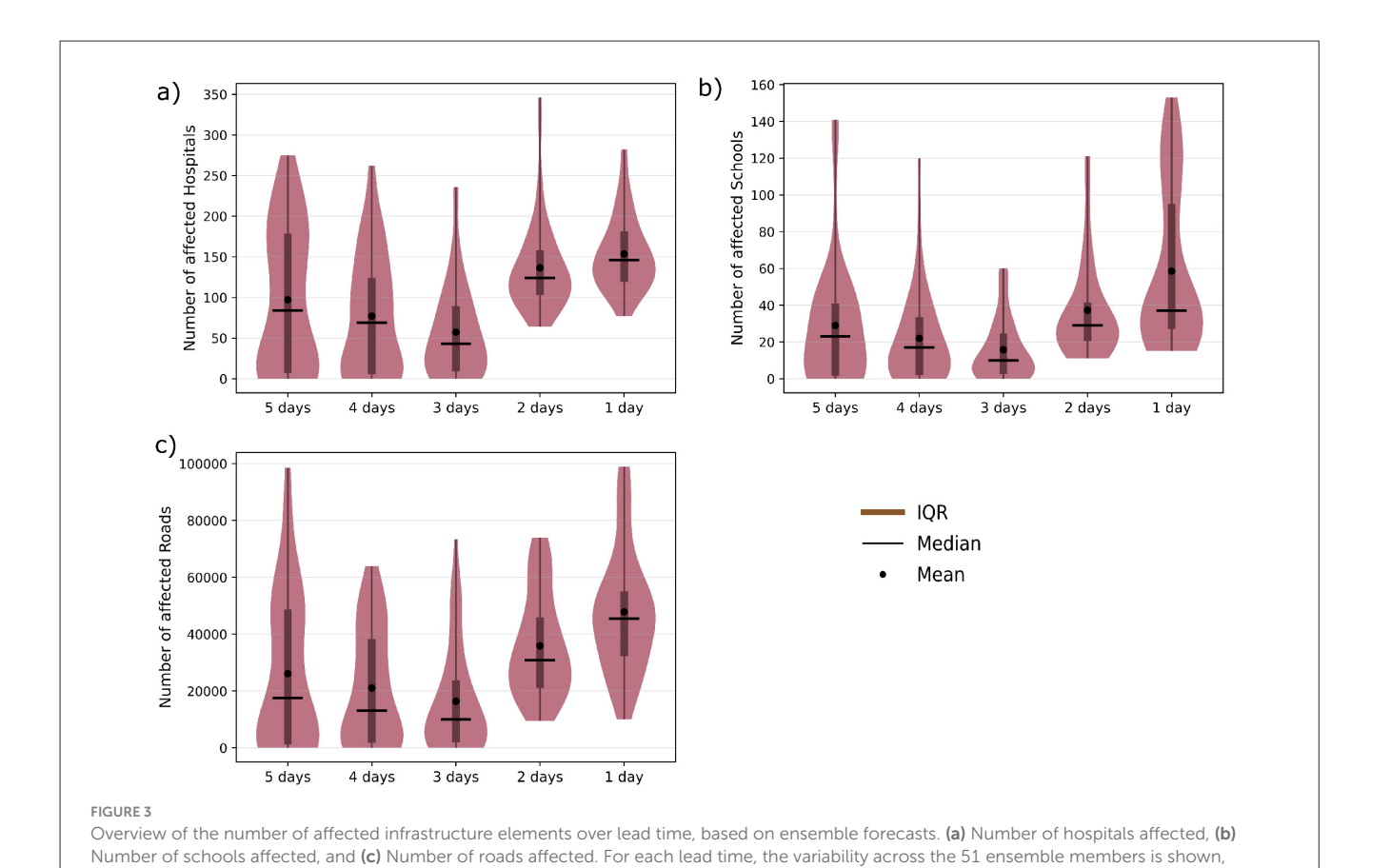
connectivity when primary-roads are disrupted. Figure 4 illustrates which hospitals, schools, or roads may potentially be disrupted one day before cyclone landfall. These visualizations offer valuable insights, highlighting critical infrastructure and specific regions that should be prioritized in disaster preparedness and response efforts. Additional visualizations for TCs Idai and Kenneth are included in Supplementary Figures S6 and S7, respectively.

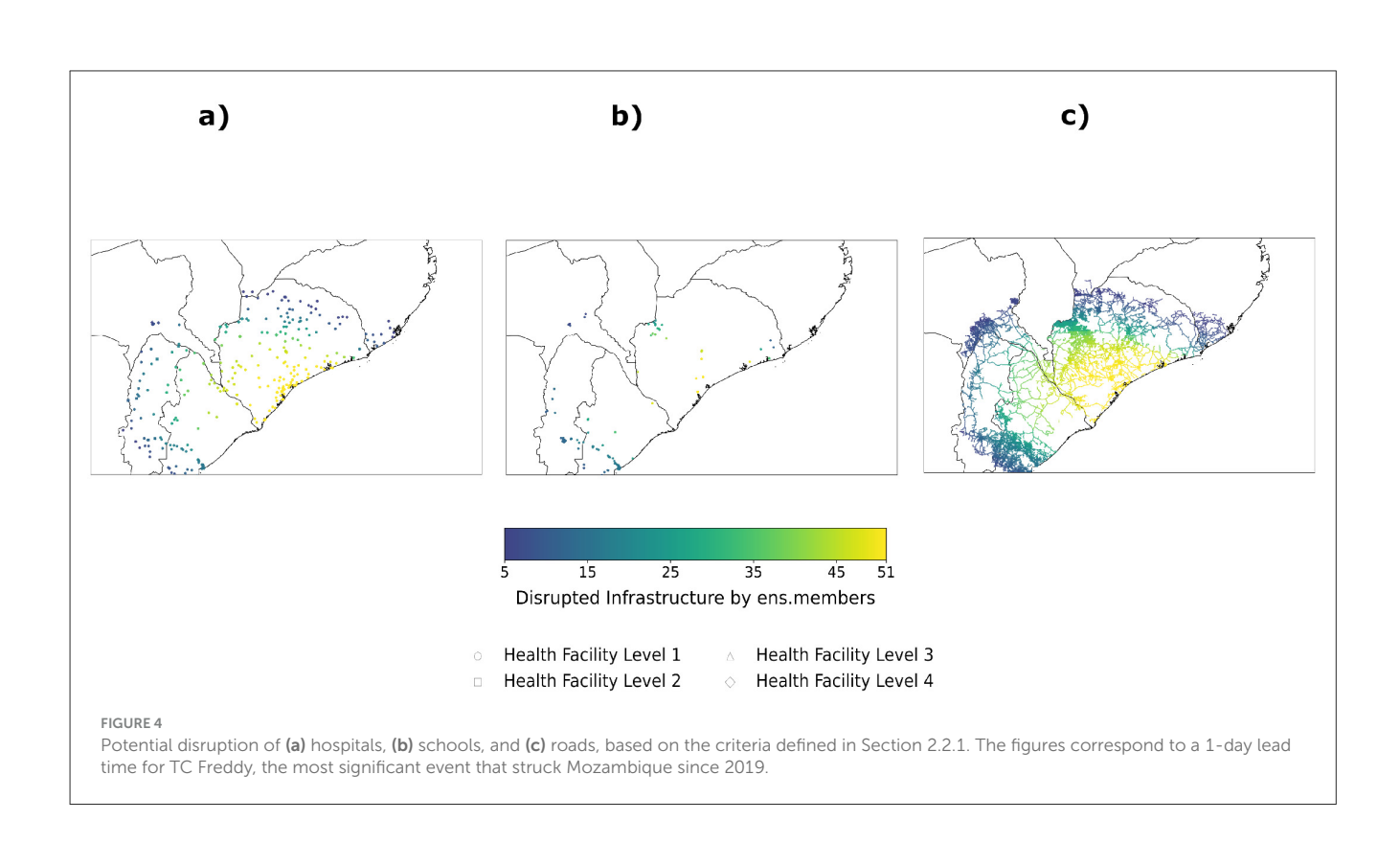
Figure 5 details the population potentially affected by service disruptions using the nearest-neighbor method. The signal is non-monotonic across lead times: it is high at longer lead time, drops to a minimum around +3 days, and intensifies again at +1 day before landfall. The province ranking also shifts at +5 days Nampula, Zambezia, and Sofala appear prominent, whereas by +1 day Nampula no longer shows service-disruption impacts while Zambezia show more impacts. These fluctuations are consistent with forecast uncertainty propagated along the IBF value chain and with TC Freddy having undergone six rapid-intensification episodes, complicating track and intensity prediction.

Consistent with this evolution, +3 days before landfall very few locations met the disruption criteria of Section 2.2.1, yielding minimal affected population across hospitals, schools, and roads. One day before landfall, the number of people potentially affected by service interruptions rises sharply. While the number directly exposed to strong winds is considerable, indirect impacts loss of access to health, education, and transport–can amplify

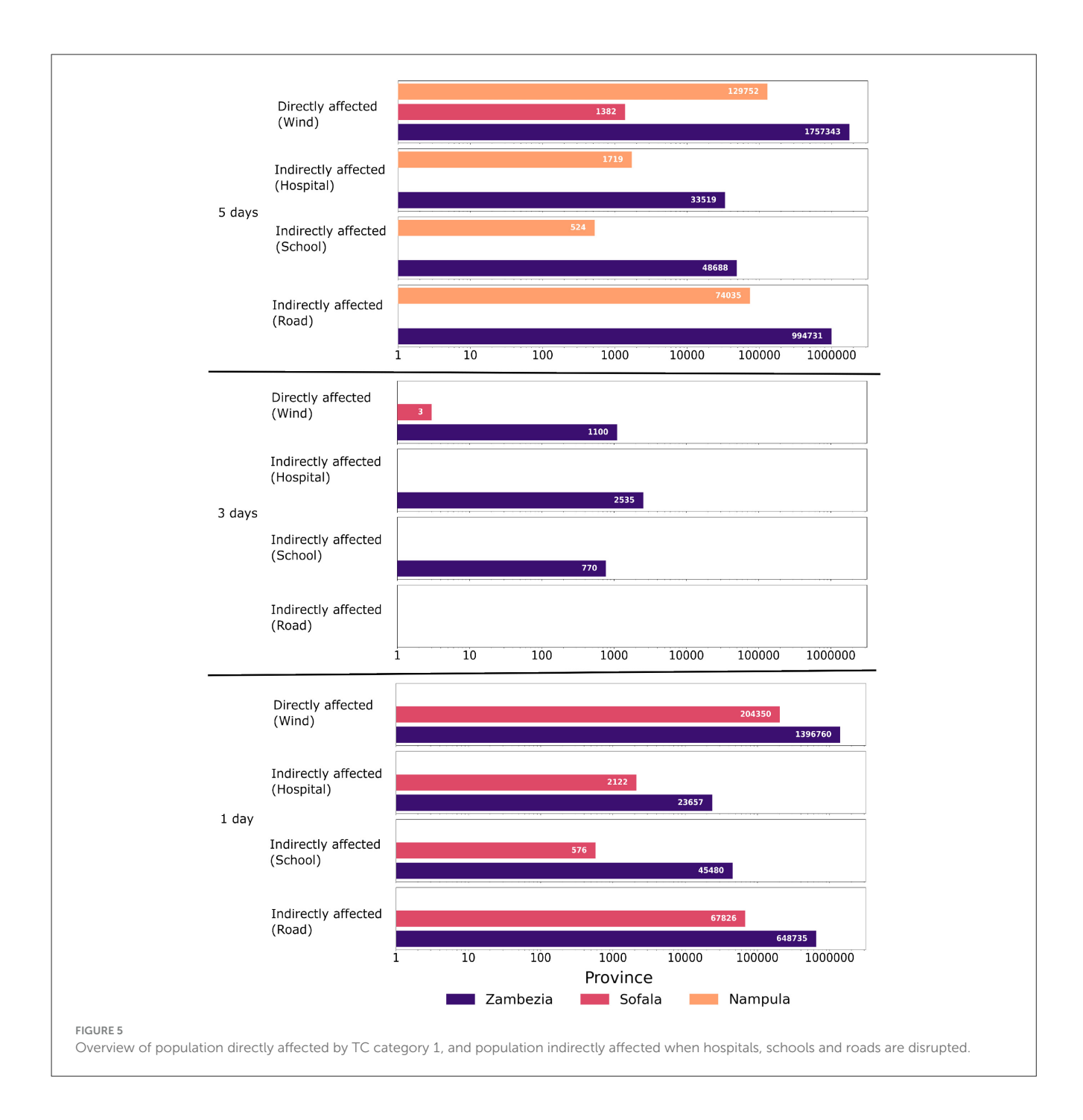
vulnerability. For example, an injury that is survivable under normal conditions may become life-threatening if hospital access is impeded by damage or blocked roads. Such indirect effects are often more spatially localized than the wind field but can critically limit access to essential services exactly when they are most needed.

Although the most severe impacts occurred in Zambezia (Figure 5), disruptions to basic services were also likely in neighboring Sofala and Nampula provinces. One day before landfall, substantial impacts were already evident: about 1,396,760 people in Zambezia and 204,350 in Sofala were in areas meeting the disruption criteria of Section 2.2.1. These totals include both direct exposure and indirect loss of access. Using the nearestneighbor method (Section 2.2.1), we estimate that, of the 1.4 million people in Zambezia at +1 day, roughly 23,657 could face reduced access to healthcare (hospital disruptions), 45,480 to schooling (school disruptions), and 648,735 to mobility (roadnetwork disruptions). This dominance of road-related indirect impacts reflects the spatial logic of the system: hospitals and schools are spatially discrete with localized service areas, whereas the road network is spatially extensive, so small disrupted segments can hinder access for large populations. Overall, indirect impacts remain smaller than direct exposure, with roads contributing most to the indirect component. Therefore, maintaining road access is pivotal to avoid secondary losses or a cascading effect. Similar overview of the direct and indirect impacts for TCs Idai





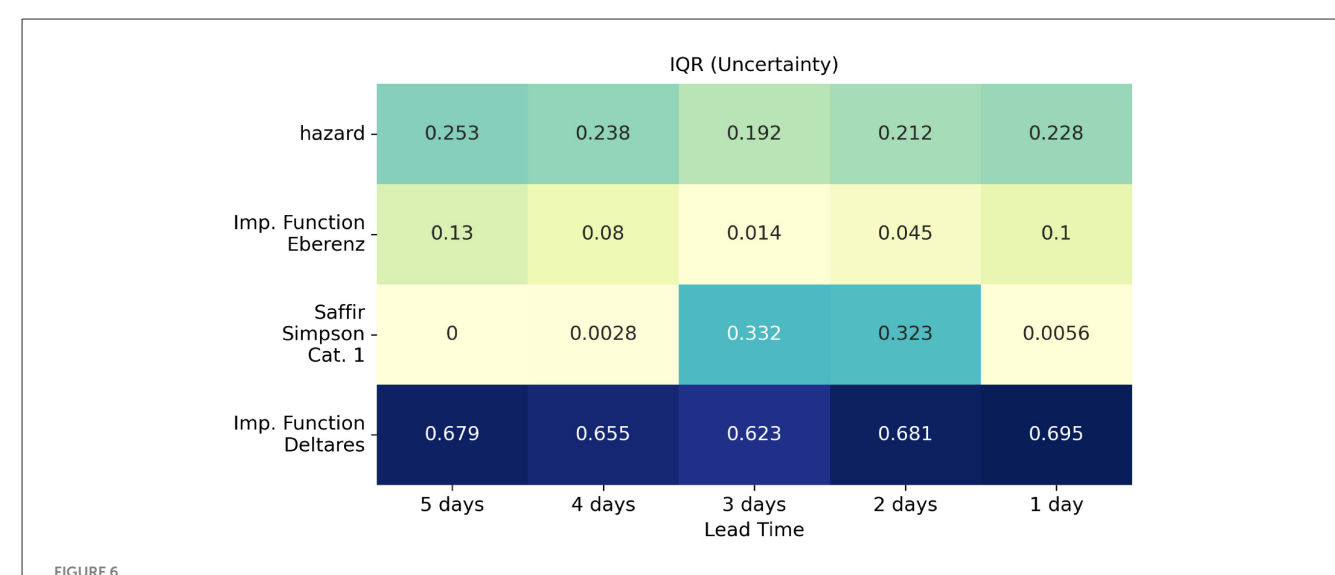
highlighting the range (e.g., mean, median, min, and max) of the predicted impact on critical infrastructure.



and Kenneth is provided in Supplementary Figures S9 and S10, respectively. The results reported here use the thresholds in Section 2.2.1 ( $T_{\rm sd}=0.20,\,A=0.10$ ). A sensitivity analysis shows that raising  $T_{\rm sd}$  to 0.50 removes pre-landfall disruption signals for TC Freddy, showing that threshold choice strongly controls earlywarning signals (Supplementary Figure S8). Therefore, transparent communication of threshold choices, and the associated trade-offs for stakeholders is pivotal.

The spatial variability across TCs Freddy, Idai, and Kenneth significantly influenced the number of people affected, as each TC impacted different regions of Mozambique. Despite these regional differences, a comparison across the three cyclones reveals key

distinctions in both direct and indirect impacts. Among the three TCs, Idai resulted in the highest overall impact, particularly with regard to indirect effects on access to healthcare, education, and road infrastructure (see Supplementary material S11). Although a standardized five-day lead time was selected as the basis for the Early Action Protocol (EAP) assessment, the actual availability of cyclone forecast data varied between events. For TC Idai, ensemble forecast data, became available only four days before landfall. In the case of TC Kenneth, the forecast track labeled "Kenneth" was not detectable until just one day before landfall. This discrepancy does not stem from an arbitrary choice of lead time but reflects limitations in the historical forecast data from



Normalized uncertainty across the impact-based value chain from hazard to impact covering the period from five days before landfall to the day of landfall.

the ECMWF ensemble system. As a result, while TC Freddy could be analyzed from five days in advance, the analyses for TCs Idai and Kenneth begin from the earliest time the storm became identifiable in ensemble forecasts. Despite its shorter lead time, TC Idai caused widespread infrastructure disruptions, highlighting the severity of its indirect impacts. TC Freddy, with the benefit of a full five-day forecast window, also produced substantial disruptions, particularly due to its prolonged duration over the region. In contrast, TC Kenneth detected only one day before landfall led to comparatively lower levels of indirect impact across all types of exposure. However, TC Kenneth was included in the analysis because it struck shortly after TC Idai, affecting a population that had not yet recovered from the previous disaster. These differences illustrate how forecast lead time, storm intensity, and regional vulnerabilities collectively influence the extent of indirect impacts. They further underscore the critical role of early warning systems and impact-based forecasting in improving disaster preparedness and response.

## 3.3 Uncertainty across the value chain

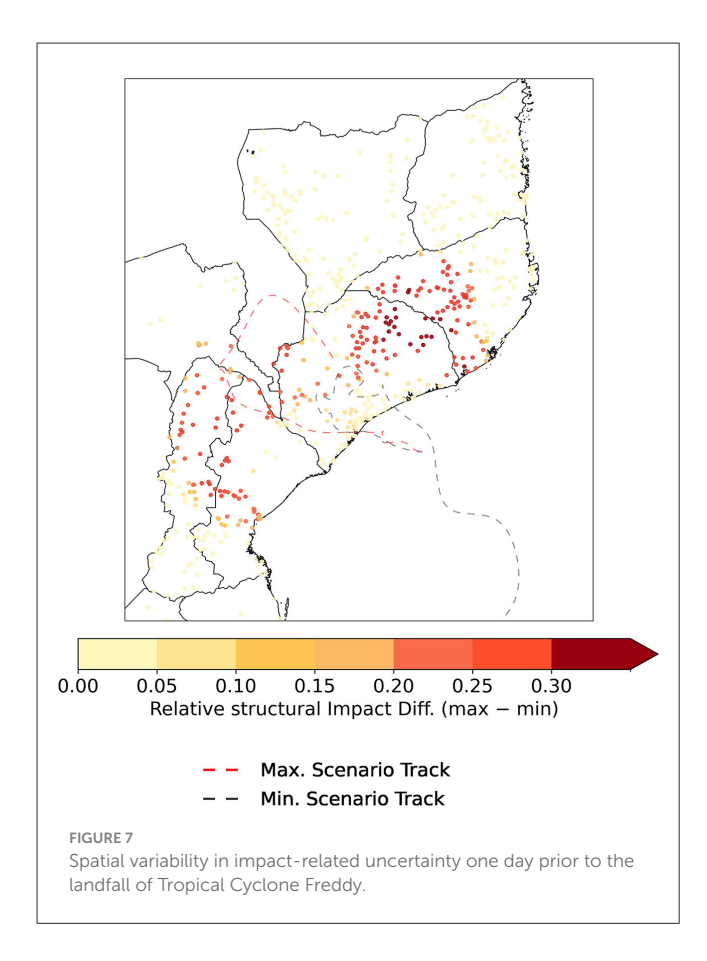
Impact-based forecasting has traditionally focused on uncertainty stemming from meteorological forecasts, often overlooking the fact that uncertainty can accumulate and propagate through subsequent stages, from hazard characterization and exposure assessment to final impact estimation. To better understand this propagation, Figure 6 presents the evolution of uncertainty (measured as the interquartile range, IQR) in different components of the impact chain and in multiple lead times for the case study of TC Freddy. To allow meaningful comparison between stages, all values were normalized. The detailed steps and equations used in the normalization and statistical processing can be found in the Supplementary material in Section 1.2. The heatmap in Figure 6 reveals that the greatest uncertainty is associated with the

vulnerability function provided by Deltares. This is expected, as the Deltares function is defined by a stepwise structure with abrupt thresholds, which can amplify variability in impact estimates. In contrast, the vulnerability function from Eberenz displays considerably lower uncertainty across all lead times due to its continuous, monotonous shape. Meteorological uncertainty, represented by the hazard layer, is highest five to four days before landfall but decreases as the event approaches, indicating increased forecast confidence closer to landfall. The Saffir-Simpson Category 1 thresholds show moderate variability, while the uncertainty associated with exposure data remains relatively low. Overall, this analysis highlights the importance of considering not just meteorological uncertainty but also the compounding effects of vulnerability and exposure in impact-based forecasts.

Building upon this, Figure 7 explores how uncertainty translates into spatial variability in modeled impacts across Mozambique. Additionally, it shows the ensemble spread of hospital impacts, computed as the maximum minus minimum mean impact across members at a 1-day lead. Along the Zambezia, Sofala coast the spread is small, indicating similar outcomes across scenarios, whereas inland areas exhibit a larger spread, highlighting where preparedness decisions are most sensitive to forecast changes. The tracks in Figure 7 illustrate this divergence: the red dashed (maximum) track crosses the country almost east-west, while the gray dashed (minimum) track originates farther south, makes landfall in Sofala, turns inland, and then recurves toward the Indian Ocean. Providing this scenario-based uncertainty hours before landfall offers decision-makers actionable spatial signals to prioritize some contingency plans.

#### 4 Discussion

The value chain of impact-based forecasting presented in this study demonstrates the added benefit of translating meteorological forecasts into impact metrics. Communicating metrics such as



impact severity, potentially disrupted hospitals, and populations directly or indirectly affected by essential service disruptions provides more detailed and operationally relevant insights than traditional forecasts alone. For the impact calculations, we used forecast track data from ECMWF, combined with population data from WorldPop and a comprehensive set of vulnerability functions. These datasets were integrated into the CLIMADA platform, an open-source tool for risk assessment. The setup was implemented retrospectively for five days prior to landfall, reflecting the structure of Early Action Protocols (EAPs), which typically initiate monitoring five days ahead of a potential event. The activation of early actions, however, is usually discussed around three days before landfall, depending on whether a predefined trigger is met (Mozambique Red Cross and IFRC, 2021).

The method presented here is designed to support flexible forecasting at any required lead time within this five-day window. In real-time applications, it allows for day-to-day impact calculations, providing timely information to decision-makers as forecast data evolves. To demonstrate its applicability and assess how early action varied between events, we modeled the impacts of the most relevant TCs affecting Mozambique: Cyclones Idai and Kenneth, both in 2019, and Cyclone Freddy in 2023. Furthermore, all components of this workflow are fully open-source and can be tailored to user needs including the risk model, input data, and the scripts used for the impact computations and visualizations presented here.

IBF still faces several research gaps, as identified in recent review studies. One key limitation is the insufficient understanding of how warning information must be tailored considering spatial, temporal, and societal dimensions to effectively trigger early actions. Methods and techniques need to be developed in close collaboration with stakeholders to ensure effective use of impactbased warnings. Furthermore, limited attention has been paid to the integration of indirect or secondary impacts, as well as cascading and compounding hazards, which are essential to complete the analytical framework (Potter et al., 2025). This study contributes to addressing one of these key gaps by integrating secondary or indirect impacts into the impact-based forecasting value chain. Previous research has emphasized that disruptions to healthcare services are not only a result of physical damage to infrastructure but also of the limited accessibility faced by populations, particularly in low-density areas. In Mozambique, for example, hospitals with high service coverage are primarily concentrated in urban centers, while rural communities often face travel times of at least 45 minutes to several hours on foot to reach the nearest facility. To mitigate this vulnerability, mobile health units are deployed to provide basic services such as vaccination programs. However, during Tropical Cyclone Freddy, flooding severely affected these mobile health services, leading to interruptions in vaccination campaigns that persisted for weeks or even months (Rossi et al., 2024; Hierink et al., 2020). Although spatial data on the precise locations of mobile units was not available for this study, we argue that such disruptions constitute a critical form of indirect impact with substantial implications for public health. Similar patterns were observed in the aftermath of TCs Idai and Kenneth. These events damaged health facilities and caused secondary effects such as increased travel times and reduced coverage of healthcare. Following TC Idai, the proportion of children under five years of age with access to a healthcare facility in two hours decreased from 78. 8% to 52. 5%. In areas affected by TC Kenneth, accessibility declined from 82.2% to 71.5%, leaving approximately 14,330 children without adequate access to care (Hierink et al., 2020). These cases underscore the importance of forecasting not only direct exposure to hazards, but also the likelihood of healthcare service disruptions and their broader societal consequences.

The methodology presented here seeks to operationalize this understanding by incorporating such effects into the impactbased forecasting framework. As shown in Figure 5, estimating the population that might be disrupted by wind speed provides critical insight into direct exposure. However, identifying populations whose access to essential services such as hospitals is hindered by infrastructure disruptions offers an additional and equally important perspective. For example, areas with populations located below the defined thresholds of physical disruption or in less densely populated regions may still experience service interruptions due to damage to nearby healthcare facilities or increased travel times. As a result, these populations, although not located in high-exposure zones, may still suffer limited access to critical services, with potentially severe public health consequences. This situation was clearly observed in the case of TC Freddy, as illustrated in Figure 5, where populations outside the strongest wind zones experienced significant disruptions to

healthcare access. These findings emphasize the importance of extending IBF approaches to include indirect impacts, particularly for under-served or remote communities that are highly vulnerable to service disruptions.

The case studies of TCs Idai, Kenneth, and Freddy aim to identify the evolution of early action protocols in Mozambique. During Cyclones Idai and Kenneth in 2019, an early warning system was in place; however, coordination to disseminate timely information and provide guidance on how to respond was limited. Formal early action plans and predefined triggers were still under development or completely absent at that time. In the case of Cyclone Idai, the Zimbabwe Meteorological Office issued a warning in advance. Nevertheless, it was insufficient to support the relocation of at-risk populations. Logistical arrangements were lacking, there were no designated shelters for communities, and the population did not know how to respond. A critical intermediary mechanism to translate warnings into understandable and actionable consequences was missing (ReliefWeb, 2019). Even when communities were aware that a TC was approaching, many assumed it would be similar to past events and therefore did not take precautionary measures. This highlights a significant communication gap in impact-based forecasting specifically, the need to effectively convey the difference between an event with 60 km/h wind speeds and one with 180 km/h winds (ReliefWeb, 2021). Lessons learned from Cyclones Idai and Freddy, along with the development of the EAPs established through partnerships among local and national organizations and the German Red Cross have led to the implementation of mechanisms for activating anticipatory actions. A mapping of authorized actions has also been performed in relevant sectors to ensure effective communication flows and that each responsible entity receives the necessary information to act. These protocols, which include threshold values for triggering actions, were developed using 30 years of historical data to establish scientifically grounded activation criteria (International Federation of Red Cross and Red Crescent Societies, IFRC). Evidence from communities exposed to anticipatory action during Cyclone Freddy shows that they received warnings earlier and were more likely to believe that the event would occur. While some residents took precautionary measures, others still experienced uncertainty about how to respond. In contrast, communities not reached by anticipatory actions received warnings with less lead time and showed lower levels of trust in the information (Malawi Red Cross Society and Danish Red Cross, 2024). This highlights the importance of improving the communication flow by including impact-based triggers. Such triggers can inform the population not only about the hazard itself but also about the potential consequences such as the loss of access to health services. Contingency plans can be activated to ensure the availability of alternative health facilities or sectors to maintain essential services like health care or preserving for example medicaments and vaccination dosis.

IBF links forecasts to impacts, yet many implementations rely on computationally heavy physics-based chains or surrogate models that trade accuracy and transferability especially outside their training domain (Najafi et al., 2024). A central gap is uncertainty: IBF depends on input data and assumptions at multiple stages, so end-to-end propagation and clear representation

of impact uncertainty are essential. Probabilistic approaches are better suited than deterministic ones for extreme events and anticipatory action, but choices must match the use case and data. Following Kam et al. (2024), we treat each ensemble member as a distinct meteorological realization and pair this with alternative vulnerability curves. In our study, the full 51-member ECMWF ensemble and multiple vulnerability curves yield min/median/max counts of disrupted hospitals, schools, and roads, plus associated affected populations; we also tested disruption and alert threshold combinations for indirect-impact sensitivity. Finally, a normalized IQR analysis (Figure 6) traces uncertainty across hazard, vulnerability, and exposure, showing that relative contributions shift with lead time.

We now detail each component of the IBF chain. Hazard forecast: In the case of TC Freddy, one of the most significant sources of uncertainty stemmed from the ECMWF forecast. The model underestimated Freddy's intensity, exhibited a considerable mean track error, and predicted premature dissipation by not accurately recording the full development of the cyclone (Liu et al., 2023).

Vulnerability: In contrast, we hypothesize that uncertainty introduced by the vulnerability functions was comparatively lower. This is evident in the vulnerability function by Eberenz (Figure 6), which shows low variability compared to the Deltares vulnerability function, indicating a smaller contribution to overall uncertainty in this specific case. However, uncertainties in vulnerability can vary from event to event. In situations where forecasts are relatively accurate, local vulnerability estimates may contribute more significantly to overall model uncertainty. This insight aligns with findings from recent research in the Philippines, where an IBF model for housing damage using XGBoost showed that removing local vulnerability data and relying solely on global features did not negatively affect performance. In fact, the model achieved higher true-positive rates and reduced false negatives and false positives, thus minimizing unnecessary early actions.

Disruption threshold: We flag structural disruption at impact ≥ 0.20, adopting the lower bound of the severe impact class in Richter et al. (2018). At this level, expected wind effects align with Saffir-Simpson descriptors [e.g., roof failure, major envelope damage, blocked access; (National Hurricane Center, 2023)]. In Mozambique, post-Idai assessments reported tearing roofs off homes and buildings, the Beira Central Hospital emergency room rendered non-functional, and widespread road and bridge outages with power interruptions (ReliefWeb, 2019). Given this context, 0.20 is a conservative cut-off that reduces missed disruptions. In line with this concern about missed events, a stricter 0.50 threshold identified no disrupted infrastructure at any lead time before landfall for TC Freddy, thereby missing disruption signals. Alert threshold: We set the alert threshold at impact  $\geq 0.10$  to prioritize preparedness. In access-constrained settings (single road access), the cost of a missed event is high; a lower alert share increases recall and triggers earlier warnings, even at the expense of more false alarms. Where logistics are stronger and rapid on-site mobilization is feasible, a higher alert share may better focus resources on the most affected assets. In practice, this is an operational parameter that users can tune to their priorities. Trade-offs and lead time: Sensitivity analysis (Supplementary Figure S8) indicates that the

disruption cut-off  $T_{sd}$  is the primary lever-raising it from 0.20 to 0.50 collapses pre-landfall signals. By contrast, changing the alert share A has a smaller effect: lowering A adds alerts at locations where only a few ensemble members exceed  $T_{\rm sd}$ , and raising A removes these borderline cases; the main hotspots remain largely unchanged compared with the choice of  $T_{\rm sd}$ . Differences between threshold pairs become more pronounced as landfall approaches, suggesting preventive settings (e.g.,  $T_{sd}$ =0.20, A=0.10) early in the EAP window and tighter settings closer to impact, according to operational priorities. Exposure: Data on critical infrastructure extracted from OpenStreetMap is represented by point features and line-strings. While this dataset is widely used, there is some uncertainty regarding the precise locations of certain infrastructure elements, which may be slightly offset from their actual positions. Although our model accounts for these spatial inaccuracies, they are expected to have minimal influence on the overall uncertainty of the model.

Critical infrastructures, for example, schools, hospitals, and primary roads-face rising climate-driven extremes, yet many CI models remain data-intensive, local, and hard to transfer, and hazard models often stop at direct asset damage, overlooking interdependencies. To bridge this gap, we present an opensource, impact-based forecasting pipeline that converts ECMWF tropical-cyclone forecasts into decision-ready metrics on both asset disruption and basic service loss. Implemented in CLIMADA, it captures interdependences between infrastructure and population and operates over a five-day Early Action Protocol horizon with daily updates. Thresholds are conservative and tunable: a 0.20 disruption cut-off reduces missed disruptions, and a 0.10 alert share prioritizes preparedness; a sensitivity check on TC Freddy showed that raising the disruption cut-off to 0.50 identified no pre-landfall disruptions, whereas 0.20 retained clear ensemble signals. Its modular, lightweight design and reliance on open hazard, exposure, and vulnerability data make the pipeline transferable across geographies and hazards and suitable for routine anticipatory planning.

# Data availability statement

The original contributions presented in the study are included in the article/Supplementary material, further inquiries can be directed to the corresponding author.

## **Author contributions**

GE: Conceptualization, Data curation, Formal analysis, Investigation, Methodology, Visualization, Writing – original draft, Writing – review & editing. ZS: Conceptualization, Methodology, Writing – review & editing. EM: Conceptualization, Methodology, Writing – review & editing. TR: Writing – review & editing. SB: Writing – review & editing. DB: Resources, Writing – review & editing. AZ: Writing – review & editing.

# **Funding**

The author(s) declare that financial support was received for the research and/or publication of this article. Open Access funding was provided by the University of Bern.

# Acknowledgments

This work was initiated in the framework of the Weather4UN pilot project, through which Switzerland, via MeteoSwiss, supports the development of the WMO Coordination Mechanism (WCM). The WCM aims to improve access to weather and climate information and to provide expert guidance to the humanitarian community. The author also acknowledges the input and early feedback provided by colleagues at MeteoSwiss and the World Meteorological Organization, as well as by members of the Weather and Climate Risks (WCR) group at ETH Zurich, which contributed to the initial development of this multidisciplinary approach.

# Conflict of interest

The authors declare that the research was conducted in the absence of any commercial or financial relationships that could be construed as a potential conflict of interest.

## Generative AI statement

The author(s) declare that Gen AI was used in the creation of this manuscript. Grammar checking was performed using grammarly AI.

Any alternative text (alt text) provided alongside figures in this article has been generated by Frontiers with the support of artificial intelligence and reasonable efforts have been made to ensure accuracy, including review by the authors wherever possible. If you identify any issues, please contact us.

#### Publisher's note

All claims expressed in this article are solely those of the authors and do not necessarily represent those of their affiliated organizations, or those of the publisher, the editors and the reviewers. Any product that may be evaluated in this article, or claim that may be made by its manufacturer, is not guaranteed or endorsed by the publisher.

# Supplementary material

The Supplementary Material for this article can be found online at: https://www.frontiersin.org/articles/10.3389/fclim.2025. 1666586/full#supplementary-material

# References

Aznar-Siguan, G., and Bresch, D. N. (2019). Climada v1: a global weather and climate risk xmltex/break assessment platform. *Geoscient. Model Dev.* 12, 3085–3097. doi: 10.5194/gmd-12-3085-2019

Bakkensen, L. A., Park, D.-S. R., and Sarkar, R. S. R. (2018). Climate costs of tropical cyclone losses also depend on rain. *Environm. Res. Lett.* 13:074034. doi: 10.1088/1748-9326/aad056

Balica, S., Douben, N., and Wright, N. G. (2009). Flood vulnerability indices at varying spatial scales. *Water Sci. Technol.* 60, 2571–2580. doi: 10.2166/wst.2009.183

Bresch, D. N., and Aznar-Siguan, G. (2021). Climada v1. 4.1: towards a globally consistent adaptation options appraisal tool. *Geoscient. Model Dev.* 14, 351–363. doi: 10.5194/gmd-14-351-2021

Cardona, O., van Aalst, M., Birkmann, J., Fordham, M., McGregor, G., Perez, R., et al. (2012). *Determinants of Risk: Exposure and Vulnerability*. Cambridge, New York: Cambridge University Press. doi: 10.1017/CBO9781139177245.005

CLIMADA (2023). Climada Exposures Openstreetmap Tutorial. Zurich: ETH Zurich.

Collalti, D., and Strobl, E. (2022). Economic damages due to extreme precipitation during tropical storms: evidence from jamaica. *Nat. Hazards* 110, 2059–2086. doi:10.1007/s11069-021-05025-9

Cremen, G., Galasso, C., and McCloskey, J. (2022). Modelling and quantifying tomorrow's risks from natural hazards. *Sci. Total Environm.* 817:152552. doi: 10.1016/j.scitotenv.2021.152552

Czajkowski, J., and Done, J. (2014). As the wind blows? Understanding hurricane damages at the local level through a case study analysis. *Weather Climate Soc.* 6, 202–217. doi: 10.1175/WCAS-D-13-00024.1

Dodman, D., Hayward, B., Pelling, M., Castan Broto, V., Chow, W., Chu, E., et al. (2022). Cities, Settlements and Key Infrastructure. Cambridge, New York: Cambridge University Press.

Eberenz, S., Lüthi, S., and Bresch, D. N. (2021). Regional tropical cyclone impact functions for globally consistent risk assessments. *Nat. Hazards Earth Syst. Sci.* 21, 393–415. doi: 10.5194/nhess-21-393-2021

Field, C. B., Barros, V. R., Dokken, D. J., Mach, K. J., Mastrandrea, M. D., Bilir, T. E., et al. (2014). "Climate change 2014: impacts, adaptation and vulnerability," in Part A: Global and Sectoral Aspects. Contribution of Working Group II to the Fifth Assessment Report of the Intergovernmental Panel on Climate Change (New York: Cambridge University Press).

Gheorghe, A. V., and Vamanu, D. V. (2005). On the vulnerability of critical infrastructures: "seeing it coming". *Int. J. Crit. Infrastruct.* 1, 216–246. doi: 10.1504/IJCIS.2005.006120

Global Facility for Disaster Reduction and Recovery (2023). Multi-Hazard Risk Assessment for the Schools Sector in Mozambique. Washington, DC: World Bank International.

Golding, B. (2022). Towards the "Perfect" Weather Warning: Bridging Disciplinary Gaps Through Partnership and Communication. Cham: Springer Nature.

Hierink, F., Rodrigues, N., Mu niz, M., Panciera, R., and Ray, N. (2020). Modelling geographical accessibility to support disaster response and rehabilitation of a healthcare system: an impact analysis of cyclones idai and kenneth in mozambique. *BMJ Open* 10:e039138. doi: 10.1136/bmjopen-2020-039138

Holland, G. (2008). A revised hurricane pressure-wind model. Monthly Weather Rev. 136, 3432–3445. doi: 10.1175/2008MWR2395.1

Hülsen, S., Dee, L. E., Kropf, C. M., Meiler, S., and Bresch, D. N. (2025). Mangroves and their services are at risk from tropical cyclones and sea level rise under climate change. *Commun. Earth Environm.* 6:262. doi: 10.1038/s43247-025-02242-z

International Federation of Red Cross and Red Crescent Societies (IFRC) (2023). Global Plan 2023. Geneva: IFRC.

International Federation of Red Cross and Red Crescent Societies (IFRC) (2025). Mozambique/Africa: To Coordinate Early Actions for Preparation and Response to Cyclones in Mozambique. Geneva: IFRC.

Kam, P. M., Ciccone, F., Kropf, C. M., Riedel, L., Fairless, C., and Bresch, D. N. (2024). Impact-based forecasting of tropical cyclone-related human displacement to support anticipatory action. *Nat. Commun.* 15:8795. doi: 10.1038/s41467-024-53200-w

Kooshki Forooshani, M., van den Homberg, M., Kalimeri, K., Kaltenbrunner, A., Mejova, Y., Milano, L., et al. (2024). Towards a global impact-based forecasting model for tropical cyclones. *Nat. Hazards Earth Syst. Sci.* 24, 309–329. doi: 10.5194/nhess-24-309-2024

Lazo, J. K., Hosterman, H. R., Sprague-Hilderbrand, J. M., and Adkins, J. E. (2020). Impact-based decision support services and the socioeconomic impacts of winter storms. *Bull. Am. Meteorol. Soc.* 101, E626–E639. doi: 10.1175/BAMS-D-18-0153.1

Liu, H.-Y., Satoh, M., Gu, J.-F., Lei, L., Tang, J., Tan, Z.-M., et al. (2023). Predictability of the most long-lived tropical cyclone freedy (2023) during its

westward journey through the southern tropical indian ocean. *Geophysi. Res. Lett.* 50:e2023GL105729. doi: 10.1029/2023GL105729

Lüthi, S., Fairless, C., Fischer, E. M., Scovronick, N., Armstrong, B., Coelho, M. D. S. Z. S., et al. (2023). Rapid increase in the risk of heat-related mortality. *Nat. Commun.* 14:4894. doi: 10.1038/s41467-023-40599-x

Malawi Red Cross Society and Danish Red Cross (2024). "Comparative study in the early warnings and early actions before tropical cyclone freddy in southern malawi in areas with and without previous anticipatory action programming: Quantitative data findings and analysis," in *Technical Report, Malawi Red Cross Society and Danish Red Cross*.

Mawren, D., Hermes, J., and Reason, C. (2020). Exceptional tropical cyclone kenneth in the far northern mozambique channel and ocean eddy influences. *Geophys. Res. Lett.* 47:e2020GL088715. doi: 10.1029/2020GL088715

Meiler, S., Kropf, C. M., McCaughey, J. W., Lee, C.-Y., Camargo, S. J., Sobel, A. H., et al. (2025a). Navigating and attributing uncertainty in future tropical cyclone risk estimates.  $Sci.\ Adv.\ 11:$ eadn4607. doi: 10.1126/sciadv.adn4607

Meiler, S., Mühlhofer, E., Lüthi, S., Bresch, D. N., Ottonelli, D., Ghizzoni, T., et al. (2025b). A natural hazard risk modelling approach to human displacement - frontiers & challenges.  $Environ.\ Res.\ Clim.\ 4:045001.\ doi: 10.1088/2752-5295/ae014c$ 

Ministrio da Sade - Repblica de Moambique (2007). "Plano estratgico do sector sade 2007-2012," in *Technical report, Ministio da Sade, Maputo, Mozambique*. Available online at: https://www.uhc2030.org/fileadmin/uploads/ihp/Documents/Country\_Pages/Mozambique/PlanoEstrategicoSectorSaude\_2007-2012.pdf (Accessed June 10, 2025).

Mosimann, M. (2024). From Weather Forecasts to Impact-Based Flood Warning Systems: A Modelling Perspective (Phd dissertation). University of Bern, Bern, Germany

Mosimann, M., Kauzlaric, M., Schick, S., Martius, O., and Zischg, A. P. (2024). Evaluation of surrogate flood models for the use in impact-based flood warning systems at national scale. *Environm. Model. Softw.* 173:105936. doi: 10.1016/j.envsoft.2023.105936

Mozambique Red Cross and IFRC (2021). Mozambique: Cyclone Early Action Protocol. Available online at: https://www.ifrc.org/document/mozambique-cyclone-early-action-protocol (Accessed March 24, 2025).

Mühlhofer, E., Bresch, D. N., and Koks, E. E. (2024). Infrastructure failure cascades quintuple risk of storm and flood-induced service disruptions across the globe.  $One\ Earth\ 7,714-729.\ doi:\ 10.1016/j.oneear.2024.03.010$ 

Mühlhofer, E., Koks, E. E., Kropf, C. M., Sansavini, G., and Bresch, D. N. (2023a). A generalized natural hazard risk modelling framework for infrastructure failure cascades. *Reliabil. Eng. Syst. Safety* 234:109194. doi: 10.1016/j.ress.2023. 109194

Mühlhofer, E., Stalhandske, Z., Sarcinella, M., Schlumberger, J., Bresch, D. N., and Koks, E. (2023b). "Supporting robust and climate-sensitive adaptation strategies for infrastructure networks: a multi-hazard case study on Mozambique's healthcare sector," in *Proceedings of the 14th International Conference on Applications of Statistics and Probability in Civil Engineering (ICASP14)* (Dublin: Trinity College Dublin).

Najafi, H., Shrestha, P. K., Rakovec, O., Apel, H., Vorogushyn, S., Kumar, R., et al. (2024). High-resolution impact-based early warning system for riverine flooding. *Nat. Commun.* 15:3726. doi: 10.1038/s41467-024-48065-y

National Hurricane Center (2023). Saffir-simpson Hurricane Wind Scale. Available online at: https://www.nhc.noaa.gov/aboutsshws.php (Accessed February 27, 2025).

Nyongesa, A. M., Shi, D., Li, S., and Li, Q. (2024). Influence of convective parameterization on the simulation of tropical cyclones over the south west indian ocean: A case study of tropical cyclone idai (2019). *Atmospheric Res.* 306:107461. doi: 10.1016/j.atmosres.2024.107461

O'Neill, B., van Aalst, M., Zaiton Ibrahim, Z., Berrang Ford, L., Bhadwal, S., Buhaug, H., et al. (2022). *Key Risks Across Sectors and Regions*. Cambridge, New York: Cambridge University Press.

Papilloud, T., Steiner, A., Zischg, A., and Keiler, M. (2024). Road network disruptions during extreme flooding events and their impact on the access to emergency medical services: a spatiotemporal vulnerability analysis. *Sci. Total Environm.* 956:177140. doi: 10.1016/j.scitotenv.2024.177140

Park, S., van de Lindt, J. W., and Li, Y. (2013). Application of the hybrid abv procedure for assessing community risk to hurricanes spatially. *Nat. Hazards* 68, 981–1000. doi: 10.1007/s11069-013-0674-2

Potter, S. H., Kox, T., Mills, B., Taylor, A., Robbins, J., Cerrudo, C., et al. (2025). Research gaps and challenges for impact-based forecasts and warnings: results of international workshops for high impact weather in 2022. *Int. J. Disast. Risk Reduct*. 118:105234. doi: 10.1016/j.ijdrr.2025.105234

ReliefWeb (2019). *Cyclone IDAI: Time to Reassess Disaster Management*. Geneva: United Nations Office for the Coordination of Humanitarian Affairs (OCHA).

ReliefWeb (2021). Learning From Cyclone IDAI and Cyclone Kenneth to Strengthen Early Warning Systems in Mozambique. Geneva: United Nations Office for the Coordination of Humanitarian Affairs (OCHA).

ReliefWeb (2023). Tropical Cyclone Freddy Mozambique Update - 30 March 2023. Available at: https://reliefweb.int/report/mozambique/tropical-cyclone-freddy-mozambique-update-30-march-2023 (Accessed February 27, 2025).

Richter, H., Arthur, C., Schroeter, S., Wehner, M., Sexton, J., Ebert, B., et al. (2018). Impact-Based Forecasting for the Coastal Zone: East Coast Lows. Melbourne, VIC: Natural Hazards Research Australia.

Röösli, T., Appenzeller, C., and Bresch, D. N. (2021). Towards operational impact forecasting of building damage from winter windstorms in switzerland. *Meteorol. Appl.* 28:e2035. doi: 10.1002/met.2035

Rossi, B., Formenti, B., Cerini, C., Tique, N., da Celma Cossa, R., Boniotti, F., et al. (2024). Addressing health care disruption in rural mozambique due to extreme climate events: mobile units tackling cyclones, vaccine-preventable diseases, and beyond. *Front. Trop. Dis.* 5:1328926. doi: 10.3389/fitd.2024.1328926

Schneider, M., Halekotte, L., Mentges, A., and Fiedrich, F. (2025). Dependent infrastructure service disruption mapping (disruptionmap): a method to assess cascading service disruptions in disaster scenarios. *Sci. Rep.* 15:5736. doi: 10.1038/s41598-025-89469-0

Sedhain, S., van den Homberg, M., Teklesadik, A., van Aalst, M., and Kerle, N. (2025). Evaluating impact-based forecasting models for tropical cyclone anticipatory action. *Int. J. Disast. Risk Reduct.* 2025:105782. doi: 10.1016/j.ijdrr.2025.105782

Stalhandske, Z., Steinmann, C. B., Meiler, S., Sauer, I. J., Vogt, T., Bresch, D. N., et al. (2024). Global multi-hazard risk assessment in a changing climate. *Sci. Rep.* 14:5875. doi: 10.1038/s41598-024-55775-2

Svegrup, L., Johansson, J., and Hassel, H. (2019). Integration of critical infrastructure and societal consequence models: impact on swedish power system mitigation decisions. *Risk Analysis* 39, 1970–1996. doi: 10.1111/risa.13272

United Nations Office for Disaster Risk Reduction (2015). Sendai Framework for Disaster Risk Reduction. Available online at: https://www.undrr.org/implementing-sendai-framework/sendai-framework-disaster-risk-reduction-2015--2030 (Accessed April 14, 2025).

United Nations Office for Disaster Risk Reduction (2023). Southern Africa Cyclone Freddy 2023: Forensic Analysis. Available online at: https://www.undrr.org/resource/southern-africa-cyclone-2023-forensic-analysis (Accessed March 11, 2025).

United Nations Statistics Division (2023). *Indicators List - Sustainable Development Goals*. New York, NY: United Nations.

Verschuur, J., Fernández-Pérez, A., Mühlhofer, E., Nirandjan, S., Borgomeo, E., Becher, O., et al. (2024). Quantifying climate risks to infrastructure systems: a comparative review of developments across infrastructure sectors. *PLoS Climate* 3:e0000331. doi: 10.1371/journal.pclm.0000331

World Meteorological Organization (2021). Guidelines on Multi-Hazard Impact-Based Forecasting and Warning Services—Part 2: Putting Multi-Hazard IBFWS into Practice. Number WMO-No. 1150. Geneva: World Meteorological Organization.

World Meteorological Organization (2023). Early Warnings for All: The UN Global Early Warning Initiative for the Implementation of Climate Adaptation—Executive Action Plan 2023–2027. Geneva: World Meteorological Organization.

WorldPop Project (2023). Worldpop. Available online at: https://www.worldpop.org/ (Accessed June 15, 2023).

Yarveysi, F., Jafarzadegan, K., Tripathy, S. S., Moftakhari, H., and Moradkhani, H. (2025). A data-driven framework for an efficient block-level coastal flood risk assessment. *Int. J. Disast. Risk Reduct.* 122:105478. doi: 10.1016/j.ijdrr.2025. 105478

Ye, M., Ward, P. J., Bloemendaal, N., Nirandjan, S., and Koks, E. E. (2024). Risk of tropical cyclones and floods to power grids in southeast and east asia. *Int. J. Disast. Risk Sci.* 15, 494–507. doi: 10.1007/s13753-024-00573-7